BMC Medical Imaging

RESEARCH

Open Access

Low-dose whole-spine imaging using slot-scan digital radiography: a phantom study

Shigeji Ichikawa[1,4*], Hiroe Muto[1], Masashi Imao[2], Takashi Nonaka[3], Kouji Sakekawa[3] and Yasutaka Sato[3]

Abstract

Background Slot-scan digital radiography (SSDR) is equipped with detachable scatter grids and a variable copper filter. In this study, this function was used to obtain parameters for low-dose imaging for whole-spine imaging.

Methods With the scatter grid removed and the beam-hardening (BH) filters (0.0, 0.1, 0.2, or 0.3 mm) inserted, the tube voltage (80, 90, 100, 110, or 120 kV) and the exposure time were adjusted to 20 different parameters that produce equivalent image quality. Slot-scan radiographs of an acrylic phantom were acquired with the set parameters, and the optimal parameters (four types) for each filter were determined using the figure of merit. For the four types of parameters obtained in the previous section, SSDR was performed on whole-spine phantoms by varying the tube current, and the parameter with the lowest radiation dose was determined by visual evaluation.

Results The parameters for each filter according to the FOM results were 90 kV, 400 mA, and 2.8 ms for 0.0 mm thickness; 100 kV, 400 mA, and 2.0 ms for 0.1 mm thickness; 100 kV, 400 mA, and 2.8 ms for 0.2 mm thickness; and 110 kV, 400 mA, and 2.2 ms for 0.3 mm thickness. Visual evaluation of the varying tube currents was performed using these four parameters when the BH filter thicknesses were 0.0, 0.1, 0.2, and 0.3 mm. The entrance surface dose was 59.44 µGy at 90 kV, 125 mA, and 2.8 ms; 57.39 µGy at 100 kV, 250 mA, and 2.0 ms; 46.89 µGy at 100 kV, 250 mA, and 2.8 ms; and 39.48 µGy at 110 kV, 250 mA, and 2.2 ms, indicating that the 0.3-mm BH filter was associated with the minimum dose.

Conclusion Whole-spine SSDR could reduce the dose by 79% while maintaining the image quality.

Keywords Slot-scan technology, Whole spine, Radiation dose, Beam-hardening filter, Whole spine radiography

Background

Slot-scan digital radiography (SSDR; Shimadzu, Kyoto, Japan) can remove scatter grids and automatically vary beam-hardening copper filters (BH filters). The filter material is copper, which may reduce X-rays in the low-energy region, thereby reducing the dose.

X-rays are incident perpendicular to the subject or patient such that seamless images with little distortion can be obtained, which is useful for alignment measurement in orthopedics and preoperative and postoperative evaluations. During imaging, the X-ray tube and flat panel detector move simultaneously from the head to the foot at the same speed while delivering X-rays. X-rays are delivered in the form of a beam through a narrow 4-cm slit. The X-ray preparation is completed by confirming

*Correspondence:
Shigeji Ichikawa
xpichikawafussa@yahoo.co.jp
[1] Suzuka University of Medical Science, Graduate School of Health Science Division of Health Science, 1001-1, Kishioka, Suzuka, Mie 510-0293, Japan
[2] Department of Radiology, Faculty of Health Science, Gunma Paz University, 1-7-1 Tonyamachi, Takasaki, Gunma 370-0006, Japan
[3] Department of Radiological Technology, Fussa Hospital, 1-6-1 Kamidaira, Fussa-ku, Tokyo 197-0012, Japan
[4] Graduate School of Health Science, Suzuka University of Medical Science, 1001-1, Kishioka, Suzuka, Mie 510-0293, Japan

the starting position (head side) and the ending position (foot side) with X-ray fluoroscopy. After acquisition, dozens of images acquired using the workstation are superimposed and combined into a single long image. The scatter grid is attached and detached manually, and the BH filter is controlled by a console at hand [1–7].

In general, the image quality is dependent on tube voltage, tube current, and exposure time. The auxiliary factors include scatter grids, filters, distance, and image processing. There is no fixed method to reduce the dose; however, the characteristics of the device and the tools associated with the device can be used to reduce the radiation dose [8–22]. In this study, the parameters of low-dose whole-spine imaging were investigated.

Methods

Ethical approval was obtained from the Fussa Hospital Ethics Review Committee (Number: 41). The system, phantom, and dosimeter used are shown in Table 1.

First, the scatter grids were removed, a BH filter (0.0, 0.1, 0.2, or 0.3 mm) was inserted, and the tube voltage (80, 90, 100, 110, or 120 kV) and exposure time were adjusted to create 20 different parameters that would provide equivalent image quality. The tube current was kept constant at 400 mA.

The Shimadzu Sensitivity (SS) value, which is a sensitivity index used to stabilize the density that was used in Shimadzu's equipment, was used in this study to obtain equivalent image quality. The SS values are similar to the S values used in X-ray digital imaging, but the concept differs slightly depending on the equipment of the manufacturer.

An SS value of 200 is defined as the value obtained when 2.58×10^{-7} C/kg of radiation reaches the detector at a tube voltage of 80 kV. The optimal image has an SS value of 200 to 300. In this study, the SS value was adjusted to be in the range of $250 \pm 20\%$. The 20 different parameters are listed in Table 2.

Method 1

SSDR was performed using 20 different parameters on an acrylic phantom (20 cm thick) with an X-ray chart and dosimeter probe placed on it, and images and entrance surface dose (ESD) were measured (Fig. 1; Table 1). From the images acquired, the "Mean ROI-A" and "Mean ROI-B" of the region of interest were defined in ImageJ (ver. 1.41; National Institutes of Health, Bethesda, MD), as shown in Fig. 2, and the standard deviation (SD) for noise (N) was used to obtain the contrast-to-noise ratio (CNR) (Eq. (1)).

$$\mathrm{CNR} = \frac{\text{Mean ROI-A} - \text{Mean ROI-B}}{\mathrm{SD}} \tag{1}$$

The figure of merit (FOM) was then determined for each filter using Eq. (2) to determine the best scoring parameters (four types).

$$\mathrm{FOM} = \frac{(\mathrm{CNR})^2}{\mathrm{ESD}} \tag{2}$$

FOM is a widely used tool to evaluate or compare the performance of a device, material, or procedure. As a tool for the quantitative evaluation of digital images, it is used for the comparative evaluation of X-ray equipment and parameters in the field of radiography. It is defined as the ratio of the X-ray dose to the square of the CNR, which indicates the image quality; a higher score indicates a better evaluation [23–25]. FOM was used as the slot-scan images are acquired through a narrow 4-cm slit, leading to less scattered radiation and acquisition of images that

Table 1 Slot-scan digital radiography equipment and parameters

Imaging unit	**SONIALVISION G4; Shimadzu, Kyoto, Japan**
High-voltage equipment	DR-300
Flat panel detector (inch)	17
Pixel size (μm)	139
Focus-receptor distance (cm)	110, 120, 150
Grid ratio	10
Beam-hardening filter (copper) (mm)	0.1, 0.2, 0.3
Tube voltage (kV)	40–150 (Fluoroscopy: 50–125)
Tube current (mA)	10-1000 (Fluoroscopy: 0.3–20.0)
Exposure time (s)	0.001–10.0
Density resolution (bits)	16
Whole-body phantom	PBU-60; Kyoto Kagaku, Kyoto, Japan
Dosimeter	Ray Safe X2, Unfors Ray Safe AB, Billdal, Sweden

Table 2 Measurements obtained from the imaging parameters

BH filter (mm)	Tube voltage (kV)	Tube current (mA)	Exposure time (ms)	ESD (μGy)	CNR	FOM
0.0	80	400	4.5	151.01	0.012476	10.3073×10^{-7}
	90	400	2.8	128.51	0.011805	10.8441×10^{-7}
	100	400	2.0	110.87	0.010008	9.0340×10^{-7}
	110	400	1.4	104.02	0.009008	7.8011×10^{-7}
	120	400	1.0	93.11	0.008111	7.0657×10^{-7}
0.1	80	400	6.3	118.60	0.009911	8.2829×10^{-7}
	90	400	3.2	88.99	0.008880	8.8610×10^{-7}
	100	400	2.0	69.76	0.008497	10.3496×10^{-7}
	110	400	1.6	67.13	0.006588	6.4653×10^{-7}
	120	400	1.2	62.50	0.005658	5.1221×10^{-7}
0.2	80	400	7.1	101.04	0.008222	6.6906×10^{-7}
	90	400	4.5	82.42	0.007534	6.8868×10^{-7}
	100	400	2.8	66.39	0.006834	7.0347×10^{-7}
	110	400	1.8	60.82	0.005984	5.8876×10^{-7}
	120	400	1.2	55.50	0.005572	5.5941×10^{-7}
0.3	80	400	9.0	85.55	0.006754	5.3322×10^{-7}
	90	400	5.6	72.08	0.006356	5.6047×10^{-7}
	100	400	3.2	66.01	0.006141	5.7131×10^{-7}
	110	400	2.2	60.04	0.006026	6.0481×10^{-7}
	120	400	1.4	55.99	0.005711	5.8252×10^{-7}

The tube current is constant at 400 mA on parameters

BH beam hardening, *ESD* entrance surface dose, *CNR* contrast-to-noise ratio, *FOM* figure of merit

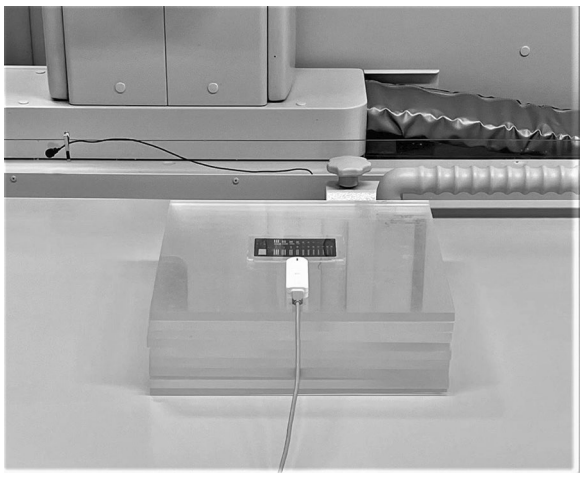

Fig. 1 The layout of slot-scan radiography with 20 different parameters is shown. The X-ray chart and dosimeter probe were placed on an acrylic phantom (20 cm thick), and slot-scan radiography was performed to obtain the chart image and dose

maintain contrast even at high voltage. Using this feature, it would be possible to find low-dose parameters by setting a high tube voltage.

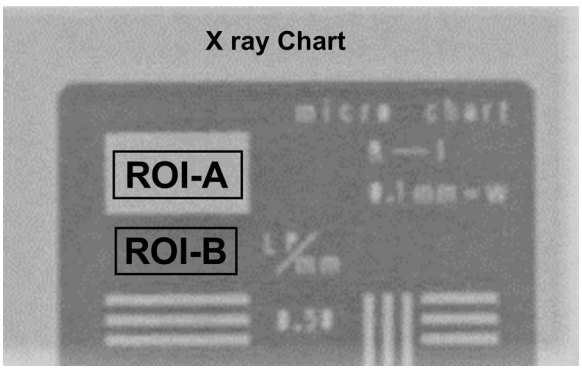

Fig. 2 Region of interest (ROI) settings for contrast-to-noise ratio (CNR) measurements. Two ROIs were established on the X-ray chart

Method 2

For each of the four parameters of each filter obtained in Method 1, the tube current was reduced to 400, 320, 250, and 125 mA, and the whole-spine phantoms were imaged for ESD and visual evaluation (Table 1).

A visual evaluation was performed using a visual analog scale (VAS) for each BH filter (Fig. 3). The VAS is a tool for objectively evaluating subjective ratings that are difficult to measure. It is one of the most frequently

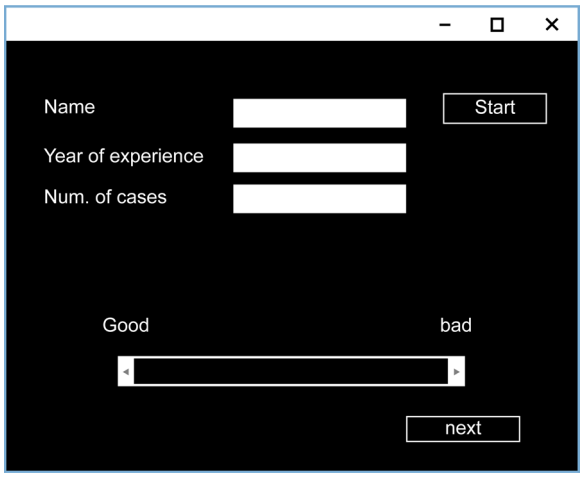

Fig. 3 Visual analog scale (VAS) used for visual assessment. Scores were given by moving the scale from good to bad (continuous confidence method). Five physicians (four orthopedic surgeons and one radiologist) oversaw the evaluation. The purpose of the test was fully explained prior to the evaluation, which was conducted in the same environment, under the same conditions (time, room light, monitors)

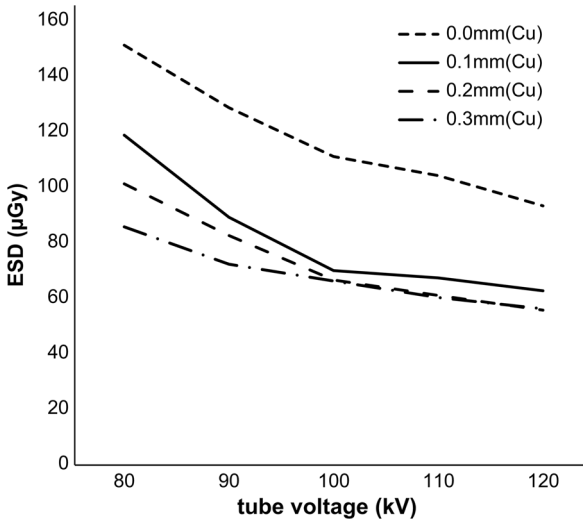

Fig. 4 Entrance surface dose (ESD) for each filter in phantom imaging with 20 different parameters

used methods in the assessment of pain [26–29]. When responding to items on the VAS, respondents select a position on a continuous line connecting two endpoints (good–bad). The specific evaluation method was based on whether the phantom was diagnostically observable from the cervical spine to the lumbar spine on imaging. The VAS scale was used to score the phantoms as "good" if observable and "bad" if unobservable. The evaluators were five physicians (four orthopedic surgeons and one radiologist) who understood and agreed with the purpose of the study. Analyses were performed by multivariate analysis (non-parametric, three-group comparison, Kruskal–Wallis test) and multiple comparisons (Steele–Drewas method) using Easy E (EZR, ver. 1.55) [30].

Results

In Method 1, the ESD was the highest at 151.01 μGy when the filter thickness was 0.0 mm and the tube voltage was 80 kV; the ESD was the lowest at 55.50 μGy when the filter thickness was 0.2 mm and the tube voltage was 120 kV, showing a decrease of about 60%. The ESD tended to decrease as the tube voltage increased (Table 2; Fig. 4). The CNR was best at 0.012476 when the filter thickness was 0.0 mm and the tube voltage was 80 kV, and it was the lowest at 0.005572 when the filter was 0.2 mm and the tube voltage was 120 kV. The CNR tended to decrease as the tube voltage between the filters increased (Table 2; Fig. 5). When the BH filter thickness was 0.0 mm, the FOM was the highest at 10.841×10^{-7} at a tube voltage of 90 kV. For a BH filter thickness of 0.1 mm, the FOM was the highest at 10.3496×10^{-7} at a tube voltage of 100 kV. For a BH filter thickness of 0.2 mm, the FOM was the highest at 7.0347×10^{-7} at a tube voltage of 100 kV. For a BH filter thickness of 0.3 mm, the FOM was the highest at 6.0481×10^{-7} at a tube voltage of 110 kV (Fig. 6). Method 2, which used the abovementioned four parameters, was considered for use since the highest score in the FOM results can be defined as the optimal parameter.

As a result of Method 2, Table 3 shows the 16 parameters obtained by reducing the tube current for the four parameters obtained from Method 1. Using these

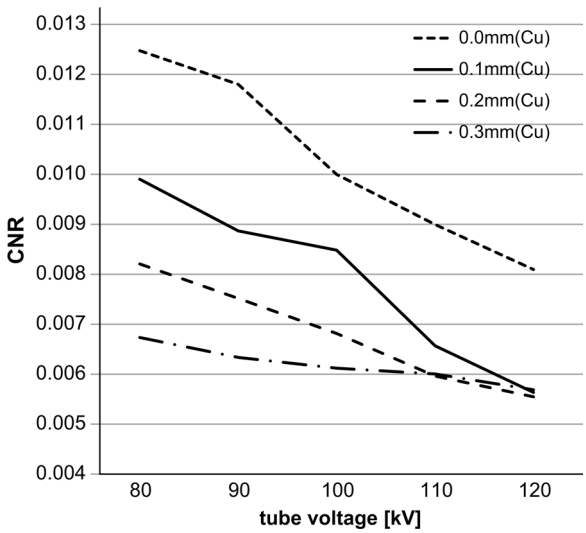

Fig. 5 Contrast-to-noise ratios (CNRs) based on 20 different parameters (X-ray chart analysis)

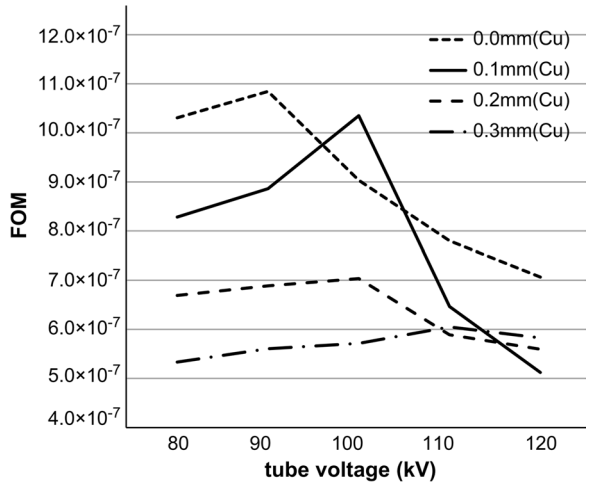

Fig. 6 ESD, CNR, and FOM obtained from 20 different parameters. ESD: Entrance surface dose; CNR: contrast-to-noise ratio; FOM: figures of merit

parameters, a whole-body phantom was photographed, and the results of the visual evaluation and dosimetry are shown in Figs. 7 and 8. In the visual evaluation, no significant difference was observed in the images with respect to the change in tube current when the filter was 0 mm ($p=0.06$). When the filter was 0.1, 0.2, and 0.3 mm, significant differences were observed in the 125-mA current range and other ranges ($p<0.05$) (Fig. 7). The ESD decreased with decreasing tube current (Fig. 8).

Discussion

The parameters obtained by FOM aim to reduce the dose by varying the tube voltage. This system is characterized by low scattered rays and good contrast images even in the high-voltage region as imaging is performed with a 4-cm wide slit; this could be the reason why the FOM results were better in the high-voltage region.

The copper filter also attenuates X-rays in the low-energy region. Typically, aluminum or copper is used to attenuate X-rays in the low-energy region. Copper has a larger atomic number and is more effective in attenuating X-rays than aluminum, thereby lowering the overall dose without changing the effective dose. Since this study was conducted in the high-voltage region, the effect of copper can be considered to be demonstrated. Furthermore, it was considered that parameters with a good balance between the image quality and dose were obtained using FOM, compared with the output obtained when the parameters recommended by the manufacturer were used in the past.

As for the radiation dose of the whole-body phantom during visual evaluation, the dose decreased at a constant rate when the tube current was decreased to 400, 320, 250, and 125 mA. This is because the tube current is proportional to the radiation dose.

Visual evaluation using the VAS showed no significant difference when the tube current was lowered if the BH filter was 0.0 mm ($p=0.06$) as the low-energy component is not removed when the BH filter is not used; therefore, it was considered that a decrease in radiation dose does not make a difference in the evaluation.

However, a significant difference ($p<0.05$) was observed at a tube current of 125 mA for 0.1-, 0.2-, and 0.3-mm BH filters. This was considered to be a significant difference at a certain boundary as the low-energy component is removed and the radiation dose is reduced. As a result, the lowest dose was obtained with a 0.3-mm BH filter (Fig. 9).

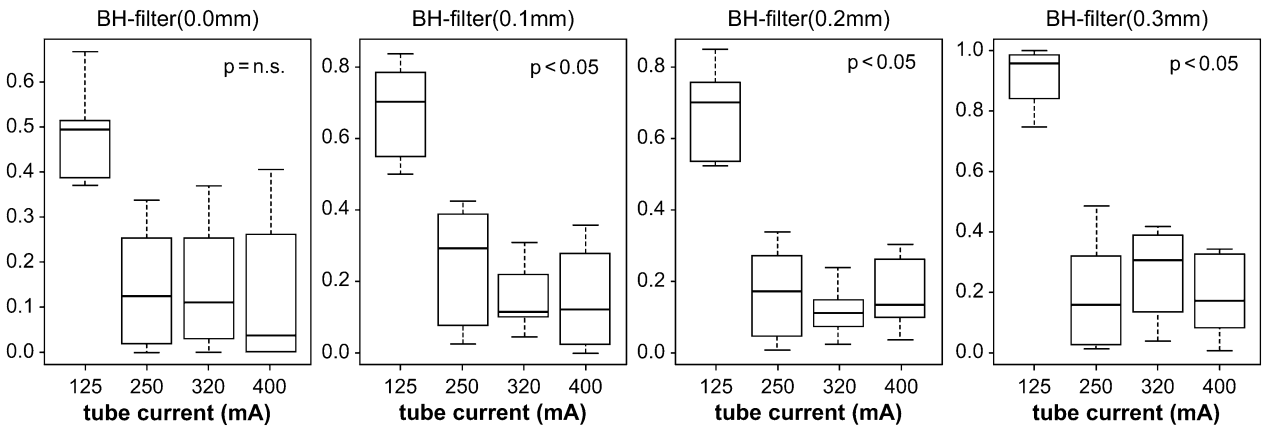

Fig. 7 Visual evaluation results for each filter. When the filter thickness is 0.0 mm, no significant difference was observed between the different tube currents. For filter thicknesses of 0.1, 0.2, and 0.3 mm, significant differences were observed for tube currents of 125, 250, 320, and 400 mA (multiple comparison, Steel–Dwass method)

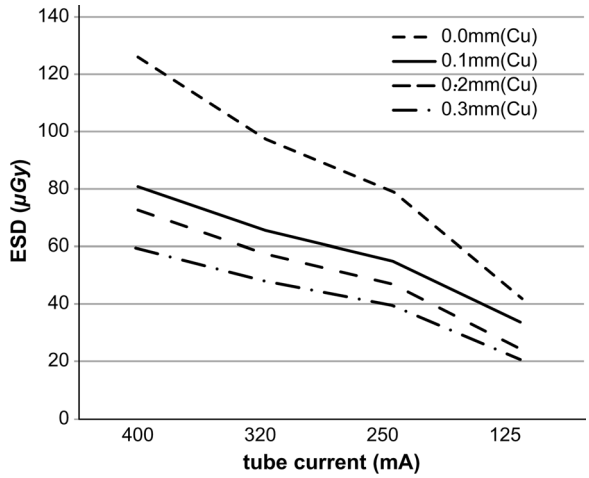

Fig. 8 Entrance Surface Dose (ESD) for the 16 parameters shown in Table 3

The lowest radiation (scatter grid uninstalled, 0.3-mm BH filter installed, 110 kV/250 mA/2.2 ms, and ESD of 39.48 μGy) dose was 79% lower than that with the parameters used in conventional examination (scatter grid installed, no filter installed, 85 kV/400 mA/6.3 ms, and ESD of 191.1 μGy; measured beforehand). In addition, there was no difference among the evaluations performed by the physicians involved in the evaluation; therefore, the validity of the evaluation result was considered guaranteed. There is no fixed method for dose reduction.

Table 3 Parameters obtained from varying tube current for each filter (16 types)

BH filter (mm)	Tube voltage (kV)	Tube current (mA)	Exposure time (ms)
0.0	90	400/320/250/125	2.8
0.1	100	400/320/250/125	2.0
0.2	100	400/320/250/125	2.8
0.3	110	400/320/250/125	2.2

BH beam hardening

Although there are many systems for imaging the entire spine, some systems make it difficult to reduce the dose as the scatter grid cannot be removed or a BH filter cannot be installed. In addition, it is assumed that some devices cannot guarantee image quality due to increased scattered radiation at high voltage settings; therefore, SSDR may be useful.

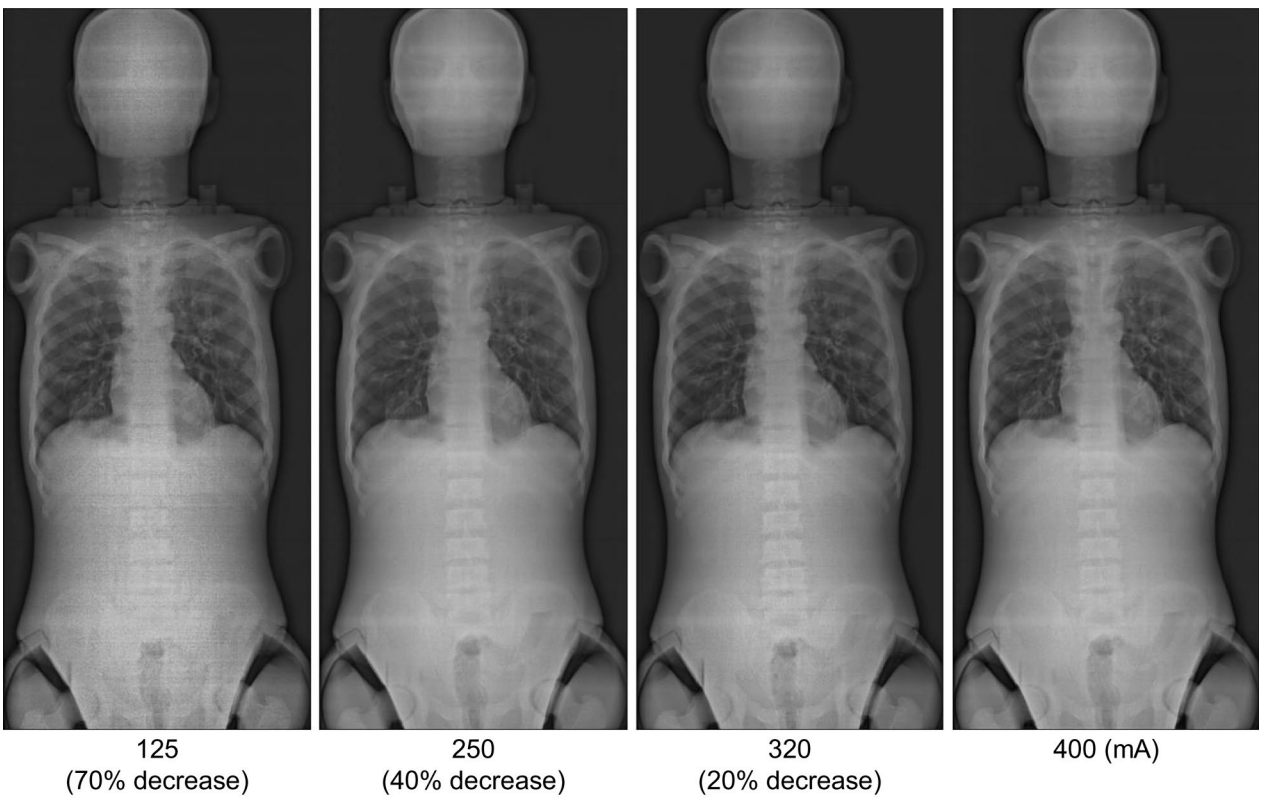

Fig. 9 Whole-spine images at a beam-hardening (BH) filter thickness of 0.3 mm. The tube currents were 400, 320, 250, and 125 mA. The tube voltage was 110 kV, and the exposure time was 1.4 ms. The lumbar spine and pelvic region are obscured at a tube current of 125 mA and can be observed at tube currents of 250, 320, and 400 mA

In addition, when considering dose reduction, it is difficult to examine the tube voltage and tube current simultaneously. Therefore, the tube voltage was examined first, and the tube current was examined based on the results of that examination. Under these circumstances, FOM is a useful tool.

Since the main purpose of whole-spine imaging is to measure the alignment and observe the entire spine, some degradation of image quality is considered acceptable. In addition, imaging is performed in all age groups and includes radiosensitive areas, such as the breast, spine, and gonads. Radiation doses should be reduced as much as possible based on the ALARA ("as low as reasonably achievable") concept. This study is effective as a dose-reduction method. However, this study does not include data based on patient-specific body shape or age, or disease-specific bone density. Therefore, its use in clinical practice requires further study. Notably, the potential for dose reduction is great, and a reduction in exposure dose is expected to significantly reduce the risk from radiation exposure.

Conclusion

Compared with conventional parameters, a 79% dose reduction was achieved when a 0.3-mm BH filter was used in this study. The image quality was determined to be the same via visual evaluation. During the imaging of the entire spine with SSDR, dose reduction can be achieved without compromising the image quality by using high voltage, low current, removal of scattering grids, and BH filters.

Abbreviations

BH	Beam-hardening
CNR	Contrast-to-noise ratio
ESD	Entrance surface dose
FOM	Figure of merit
SSDR	Slot-scan digital radiography
VAS	Visual analog scale

Acknowledgements

We thank Hiroe Muto and Koichi Shibata of Suzuka University of Medical Science for their careful guidance. We would also like to thank the staff of the Department of Radiology, Fussa Hospital, and Masashi Imao, Gunma Paz University, for their assistance with this study. We would also like to thank Editage (www.editage.com) for English language editing.

Author contributions

SI: Writing—original draft and Writing—review and editing. HM: Supervision and Project Administration. MI: Formal Analysis. TN: Methodology, Conceptualization, and Validation. KS: Validation. YS: Investigation. All authors read and approved the final manuscript.

Funding

Not applicable.

Availability data and materials

The datasets used and/or analysed during the current study are available from the corresponding author on reasonable request.

Declarations

Ethics approval and consent to participate

Ethical approval was obtained from the Fussa Hospital Ethics Review Committee (Number: 41). The requirement for informed consent was not applicable.

Consent for publication

Not applicable.

Competing interests

The authors declare that they have no competing interests.

Received: 24 October 2022 Accepted: 16 January 2023
Published online: 30 January 2023

References

1. Nash CL Jr, Gregg EC, Brown RH, Pillai K. Risks of exposure to X-rays in patients undergoing long-term treatment for scoliosis. J Bone Joint Surg Am. 1979;61:371–4.
2. Bone CM, Hsieh GH. The risk of carcinogenesis from radiographs to pediatric orthopaedic patients. J Pediatr Orthop. 2000;20:251–4.
3. Presciutti SM, Karukanda T, Lee M. Management decisions for adolescent idiopathic scoliosis significantly affect patient radiation exposure. Spine J. 2014;14:1984–90.
4. Atci IB, Yilmaz H, Antar V, Ozdemir NG, Baran O, Sadillioglu S, et al. What do we know about ALARA? Is our knowledge sufficient about radiation safety? J Neurosurg Sci. 2017;61:597–602.
5. Oakley PA, Ehsani NN, Harrison DE. The scoliosis quandary: are radiation exposures from repeated X-rays harmful? Dose Response. 2019;17:1559325819852810.
6. Ay MR, Mehranian A, Maleki A, Ghadiri H, Ghafarian P, Zaidi H. Experimental assessment of the influence of beam hardening filters on image quality and patient dose in volumetric 64-slice X-ray CT scanners. Phys Med. 2013;29:249–60.
7. Rana N, Rawat D, Parmar M, Dhawan DK, Bhati AK, Mittal BR. Evaluation of external beam hardening filters on image quality of computed tomography and single photon emission computed tomography/computed tomography. J Med Phys. 2015;40:198–206.
8. Båth M, Håkansson M, Tingberg A, Månsson LG. Method of simulating dose reduction for digital radiographic systems. Radiat Prot Dosimetry. 2005;114:253–9.
9. Busch HP, Faulkner K. Image quality and dose management in digital radiography: a new paradigm for optimization. Radiat Prot Dosimetry. 2005;117:143–7.
10. Minehiro K, Demura S, Ichikawa K, Sasagawa T, Takahashi N, Minami S, et al. Dose reduction protocol for full spine X-ray examination using copper filters in patients with adolescent idiopathic scoliosis. Spine (Phila Pa 1976). 2019;44:203–10.
11. Dobbins JT 3rd, Samei E, Chotas HG, Warp RJ, Baydush AH, Floyd CE Jr, et al. Chest radiography: optimization of X-ray spectrum for cesium iodide amorphous silicon flat-panel detector. Radiology. 2003;1:221–30.
12. Lee KH, Kwon JW, Cheol Y, Choi SH, Jung JY, Kim JH, et al. Slot-scan digital radiography of the lower extremities: a comparison to computed radiography with respect to image quality and radiation dose. Korean J Radiol. 2009;10:51–7.
13. Ranger NT, Lo JY, Samei E. A technique optimization protocol and the potential for dose reduction in digital mammography. Med Phys. 2010;37:962–9.
14. Heath R, England A, Ward A, Charnock P, Ward M, Evans P, et al. Digital pelvic radiography: increasing distance to reduce dose. Radiol Technol. 2011;83:20–8.

15. Noto K, Minami S, Morishita A, Yokoi T, Iida H, Matsubara K, et al. [Optimization of X-ray conditions for full spine X-ray examinations in slot-scan digital radiography.]. Nihon Hoshasen Gijutsu Gakkai Zasshi. 2011;67:1438–42. [in Japanese].
16. England A, Evans P, Harding L, Taylor EM, Charnock P, Williams G. Increasing source-to-image distance to reduce radiation dose from digital radiography pelvic examinations. Radiol Technol. 2015;86:246–56.
17. Ilharreborde B, Ferrero E, Alison M, Mazda K. EOS microdose protocol for the radiological follow-up of adolescent idiopathic scoliosis. Eur Spine J. 2016;25:526–31.
18. Jeon MR, Park HJ, Lee SY, Kang KA, Kim EY, Hong HP, et al. Radiation dose reduction in plain radiography of the full-length lower extremity and full spine. Br J Radiol. 2017;90:20170483.
19. Ernst C, Buls N, Laumen A, Van Gompel G, Verhelle F, de Mey J. Lowered dose full-spine radiography in pediatric patients with idiopathic scoliosis. Eur Spine J. 2018;27:1089–95.
20. Girdler S, Cho B, Mikhail CM, Cheung ZB, Maza N, Cho SK-W. Emerging techniques in diagnostic imaging for idiopathic scoliosis in children and adolescents: a review of the literature. World Neurosurg. 2020;136:128–35.
21. Williams MB, Raghunathan P, More MJ, Seibert JA, Kwan A, Lo JY, et al. Optimization of exposure parameters in full field digital mammography. Med Phys. 2008;35:2414–23.
22. Gislason AJ, Davies AG, Cowen AR. Dose optimization in pediatric cardiac X-ray imaging. Med Phys. 2010;37:5258–69.
23. Cunha DM, Tomal A, Poletti ME. Optimization of X-ray spectra in digital mammography through Monte Carlo simulations. Phys Med Biol. 2012;57:1919–35.
24. Gislason-Lee AJ, McMillan C, Cowen AR, Davies AG. Dose optimization in cardiac X-ray imaging. Med Phys. 2013;40:091911.
25. Dehairs M, Bosmans H, Marshall NW. A study of the impact of X-ray tube performance on angiography system imaging efficiency. Phys Med Biol. 2020;65:225028.
26. Revill SI, Robinson JO, Rosen M, Hogg MI. The reliability of a linear analogue for evaluating pain. Anaesthesia. 1976;31:1191–8.
27. Price DD, McGrath PA, Rafii A, Buckingham B. The validation of visual analogue scales as ratio scales measures for chronic and experimental pain. Pain. 1983;17:45–56.
28. Tang J, Guo W-C, Hu J-F, Yu L. Unilateral and bilateral percutaneous kyphoplasty for thoracolumbar osteoporotic compression fractures. J Coll Physicians Surg Pak. 2019;29:946–50.
29. Li S, Mi S, Guo R, Ma X, Han M. Application of ultrasound fusion imaging technique for unilateral percutaneous vertebroplasty in treatment of osteoporotic thoracolumbar compression fracture. J Xray Sci Technol. 2020;28:171–83.
30. Kanda Y. Investigation of the freely available easy-to-use software 'EZR' for medical statistics. Bone Marrow Transplant. 2013;48:452–8.

Publisher's Note